Journal of the European Ceramic Society 23 (2003) 195–202

www.elsevier.com/locate/jeurceramsoc

Bending strength of a PZT ceramic under electric fields

T. Fett*, D. Munz, G. Thun

Forschungszentrum Karlsruhe, Institut für Materialforschung II und Universität Karlsruhe, Institut für Zuverlässigkeit und Schadenskunde im Maschinenbau, Postfach 3640, 76021 Karlsruhe, Germany

Received 12 January 2002; accepted 1 June 2002

Abstract

Bending strength measurements were carried out in different poling states (unpoled, poled perpendicular and parallel to the specimen length axis) under various externally applied electric fields perpendicular to the specimen length axis. The main results were: (a) polarisation parallel to the specimen length axis significantly reduces strength, polarisation in the direction of thickness produces minor strength reductions only, (b) an electric field directed normal to the length axis reduces the strength. The differences caused by the poling state are discussed in terms of orientation of domains in front of natural cracks for the case of a disappearing electric field.

Keywords: Field dependent strength; Mechanical properties; PZT

1. Introduction

In the case of metallic materials, strength measurements are commonly carried out in tensile tests. The application of tensile tests to piezoelectric ceramics was demonstrated in Ref. 1. Unfortunately, the tensile test experienced serious problems in the presence of externally applied electric fields. In Ref. 1 the observation was made that in the absence of an electric field, the fracture locations were found to be equipartitioned along the specimen length, whereas in tests with externally applied electric fields strongly concentrated failure locations were found at the ends of the free specimen length. In order to avoid such disturbing influences of a special distribution of failure locations, it is recommended to perform 4-point bending tests which do not exhibit such effects.

Bending strength measurements in the presence of electric fields are reported in literature.[1–5] Unfortunately, in Refs. 2–5 the elastically computed nominal strength is given ignoring all effects of non-linearity and non-symmetry in stress vs. strain behaviour.

Among the disadvantages of using linear-elastically computed bending strength data for design purposes are their unrealistic high values which are significantly higher than those obtained from tensile tests.[6] It will be shown in this paper how the "true bending strength" can be determined.

2. Material and test arrangements

In this study, commercial-grade soft PZT (PIC 151, PI Ceramic) was investigated in bending tests at various electric fields constant with respect to time and in different states of poling: in the $\perp$-poled state (i.e. polarisation perpendicular to the specimen length axis) and in a $\parallel$-poled modification (polarisation parallel to the specimen length axis). The material with a Curie temperature of 250 °C and a density of 7.80 g/cm^3 is characterised by the manufacturer as having the dielectric constant of $\varepsilon = 2000$ and the piezoelectric coefficients of $d_{31} = -210\times10^{-12}$ m/V and $d_{33} = 450\times10^{-12}$ m/V. Measurements of Young's moduli in bending resonance tests and by ultrasonic velocity tests furnished $Y_{11}^{E} \cong 65$ GPa, $Y_{33}^{E} = 44$ GPa, $Y_{11}^{D} = 72$ GPa, and $Y_{33}^{D} = 83$ GPa.[7]

For the unpoled and the $\perp$-poled material, normal bending bars of $3\times4\times45$ mm^3 were used. All specimens (also the unpoled ones) were equipped with electrodes on the 4×45 mm^2 surfaces. In order to avoid electric

* Corresponding author.
E-mail address: theo.fett@imf.fzk.de (T. Fett).

0955-2219/02/$ - see front matter
PII: S0955-2219(02)00174-7

discharges and leakage currents at the surfaces, the specimens were covered completely with air-drying polyurethane coatings. These specimens were subjected to 4-point bending tests with the electrodes in the tensile and compression zones and the voltage applied via the metallic upper and lower loading rollers (Fig. 1a). For the ‖-poled specimens, bending bars of $3\times4\times20$ mm^3 having electrodes at the 3×4 mm^2 surfaces were used. In this case, 4-point bending tests were carried out with 16 and 8 mm roller spans. The electric voltage was applied to the electrodes via metallic springs and spheres (Fig. 1b).

3. Experimental results

The bending strengths were elastically computed from the maximum bending moment M_b and the specimens thickness B and height W according to

$$\sigma_c = \frac{6M_b}{BW^2} \quad (1)$$

Based on the relation for the failure probability, F,

$$F = 1 - \exp[-(\sigma_c/\sigma_0)^m] \quad (2)$$

the Weibull parameters, m and σ_0, were determined by the "Maximum Likelihood Procedure" according to Ref. 8.

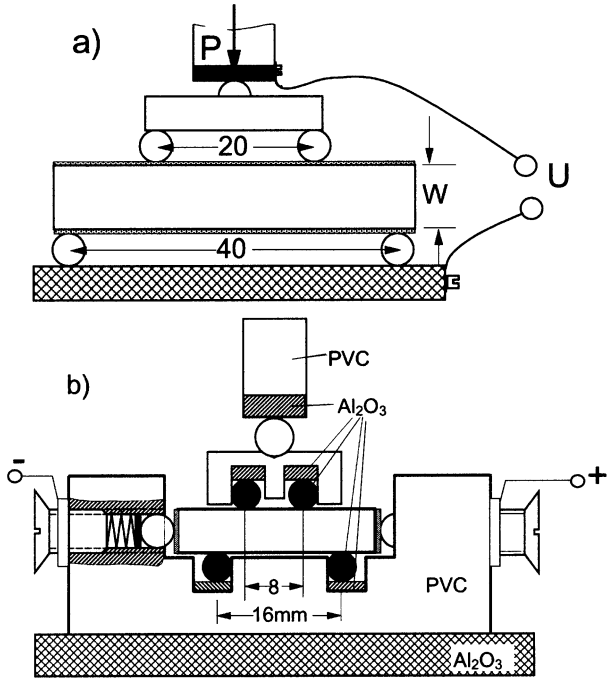

Fig. 1. Bending test arrangements: (a) for ⊥-poled specimens of 45 mm length, (b) for ‖-poled bars of 20 mm length.

3.1. Unpoled PZT

Strength measurements were carried out on the unpoled material under four electric fields of $E=1$, 0.66, 0.33 kV/mm, and $E=0$.[1] The electric field was applied for about 20 s before the specimens were loaded mechanically. The total time span between switching on the electric voltage and reaching failure stress was approximately 25–30 s. The influence of the electric field, E, on the Weibull parameter, σ_0, is shown in Fig. 2a. Impact on the Weibull exponent, m, is illustrated in Fig. 2b. The strength reduction due to the electric field becomes significant for $E=0.66$ and 1 kV/mm. Note that the same results were plotted for a positive and a negative E-field.

The 90% confidence intervals (represented by the vertical lines in Fig. 2) were computed as suggested in Ref. 8.

3.2. ⊥-Poled PZT

The strengths are represented by the Weibull distributions in Fig. 2b. Fig. 2c shows the Weibull parameters, σ_0 and m, for the bending strength of the unpoled PZT. Fig. 2d refers to the π-poled PZT as a function of the electric field applied.

A minimum scatter of strength (maximum value of the parameter m) is found near $E=-0.6$ kV/mm for the poled material and at $E=0$ for the unpoled PZT.

3.3. ‖-Poled PZT

For the tests with ‖-poled specimens, bars of 20 mm length were used. The strengths are represented by the Weibull distributions in Fig. 3a. Fig. 3b shows the Weibull parameters, σ_0, for the bending strength. Fig. 3c represents the Weibull exponent m. The 90% confidence intervals in Fig. 3b (vertical lines) indicate that the

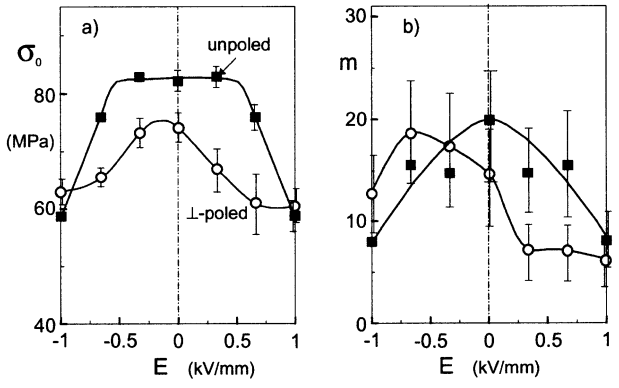

Fig. 2. Bending strengths of $3\times4\times45$ mm bars of unpoled and ⊥-poled PIC 151. Influence of the electric field on the Weibull parameters (a) σ_0 and (b) m (d); circles: ⊥-poled; squares: unpoled (after Ref. 1); vertical lines: 90%-confidence intervals.

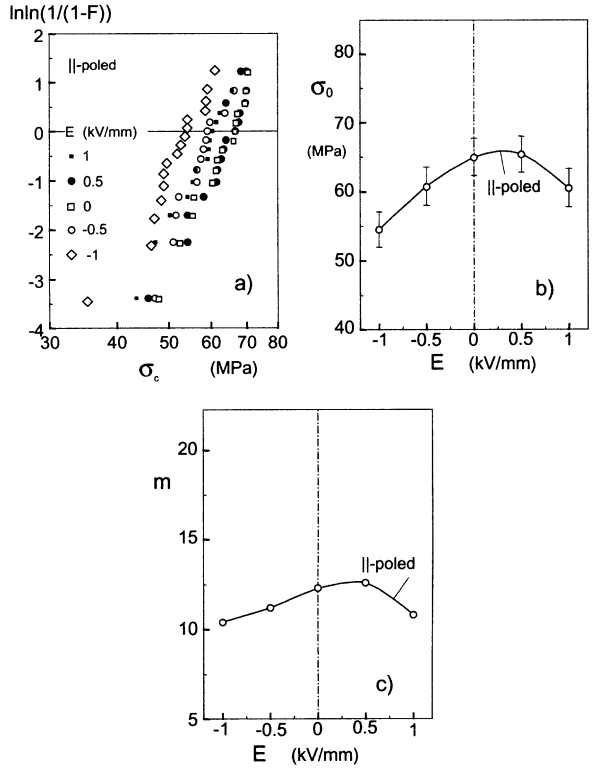

Fig. 3. (a) Bending strengths of 3×4×20 mm bars of ||-poled PIC 151. (b) Weibull parameters, σ_0 with 90% confidence intervals (b) and m (c).

changes in strength with a changing electric field are significant.

In order to allow a comparison between the results for long and short bars, the original strength data obtained for the ||-poled and the unpoled PZT with an 8 mm inner roller, here denoted as $\sigma_{c,8}$, were transformed into strength values for tests with 20 mm inner roller span, $\sigma_{c,20}$. During this the general relation for the size effect was considered, providing

$$\sigma_{c,20} = \left(S_{eff,8}/S_{eff,20}\right)^{1/m}\sigma_{c,8} \tag{3}$$

($S_{cff,8}$ = effective surface for 8mm and $S_{eff,20}$ for 20 mm inner roller span) taking into account the slightly different stress distributions along the tensile surface of the specimen according to Fig. 7.4 in Ref. 9. A comparison of the results is given in Fig. 4. In the absence of an electric field, we find the following ranking

$$\sigma_{c\parallel} < \sigma_{c\perp} < \sigma_{c,unpoled}$$

The typical influence of the electric field on the formally calculated bending strength data, namely decreasing strength for high electric fields (with asymmetry with respect to the poling direction), is in principle agreement with measurements of Makino and Kamiya[4] for the ⊥-poled PZT. The results for ||-poled PZT show a slightly

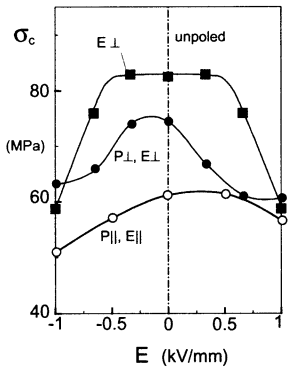

Fig. 4. Strength data for unpoled, ⊥-poled, and ||-poled PIC 151 [||-poled material re-calculated with Eq. (3)].

different behaviour compared with measurements of Fu and Zhang.[3] Whereas the 4-point bending strength for PIC 151 showed a flat maximum at positive electric field, the results of 3-point bending tests on PZT-841 reported in Ref. 3 show nearly identical effects of positive and negative fields. For unpoled materials there is a clear agreement of the field influence with literature data.[3]

4. Discussion

4.1. Influence of non-linear material behaviour on bending strength

The strength results reported before are expressed as nominal bending stress values according to Eq. (1). It is well known that PZT materials exhibit a non-linearity and non-symmetry in deformation behaviour. Consequently, the true stresses in a bending bar must deviate from elastic computations. In order to compute the true outer fibre stresses at fracture, the σ–ε curve of the PZT must be available for tension and compression. In principle, these data can be determined from tension and compression tests. Unfortunately, the electrical boundary conditions of bending tests are not sufficiently fulfilled under the homogeneous stress distributions of tensile and compression tests. As an example, it should be mentioned that in the case of ⊥-poled material, short-circuited electrodes will cause $E \neq 0$ in the bar [7], whereas in a test with homogeneous stresses $E = 0$ results. Fortunately, an appropriate procedure developed by Nadai[10] enables to determine the true outer fibre tensile stress in a bending test. The application of this method for PZT is described in detail in Ref. 11.

The true outer fibre tensile stress a results from the strains at the compressive and tensile surfaces, ε_c and ε_t, by use of Nadai's analysis as

$$\sigma = \frac{1}{6}\left(1 + \frac{d|\varepsilon_c|}{d\varepsilon_t}\right)\frac{1}{\varepsilon^*}\frac{d}{d\varepsilon^*}\left[\sigma_{nom}(\varepsilon^*)^2\right] \tag{4}$$

with

$$\varepsilon^* = (\varepsilon_t + |\varepsilon_c|)/2. \quad (5)$$

In Fig. 5a and b the influence of an electric field on the compressive and tensile strains is shown for the ⊥-poled PZT. For each curve a bending test was necessary. The ratio of the true outer fibre tensile stress to the nominal bending stress according to Eq. (1), now denoted as σ_{nom}, was determined from (4) and is plotted in Fig. 5c for varying electric fields. The true strength, defined as the true outer fibre tensile stress at fracture, is plotted in Fig. 5d together with the nominal strength data. Eq. (4) also allows to determine the strains as a function of the (true) actual stresses. These curves are given in the Appendix for unpoled and ⊥-poled material.

The corresponding results for the unpoled material are represented in Fig. 6.

Measurements with strain gauges are not an appropriate method to determine the bending strain components for ‖-poled PZT bars under high electric fields. The application of the metallic sensors on the specimen surfaces shields the electric field in that specimen region which contributes the maximum share of strains. Furthermore, electric discharges between the electrodes at the bar ends and the strain gauges have to be expected. Introducing an insulating foil between strain gauge and specimen, which has a high dielectric breakdown strength, will suppress the discharge, but also yield a reduced strain signal. Therefore, in the case of the ‖-poled PZT, the stress-strain behaviour for a disappearing electric field was determined only. The results are plotted in Fig. 7. Finally, Fig. 8 compiles the true strength values for all three material modifications.

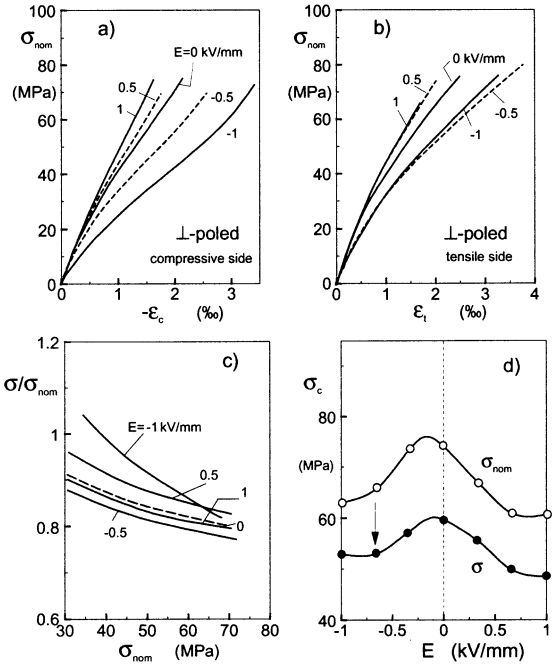

Fig. 5. Compressive (a) and tensile strains (b) in 4-point bending tests for ⊥-poled PZT; (c) ratio between true outer fibre tensile stress σ and nominal bending stress versus nominal bending stress σ_{nom}, (d) comparison of nominal bending strength and true outer fibre tensile stress.

4.2. Influence of the poling state on strength

In Table 1 the nominal and the true strength data are compiled for the special case of $E=0$. A simple explanation of these strength differences may be the influence of domain orientation in front of the crack tips. Let us consider a volume element at some distance from the tip of a natural crack. For simplicity, we consider a tetragonal

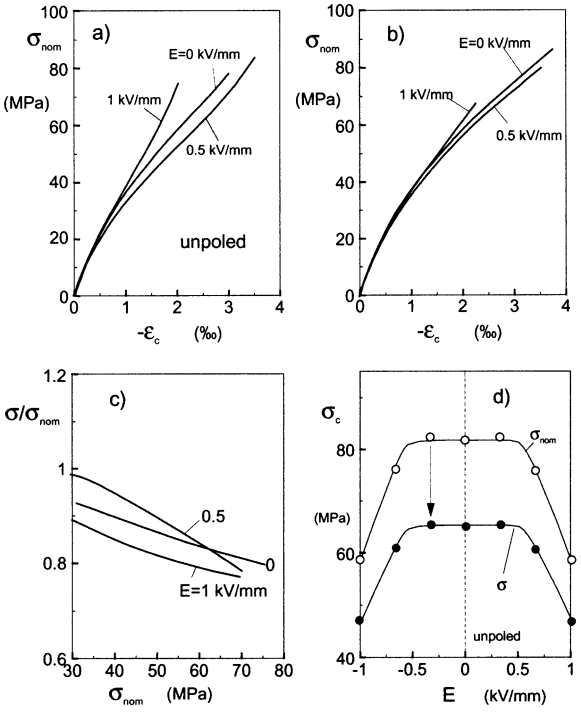

Fig. 6. Compressive (a) and tensile strains (b) in 4-point bending tests for unpoled PZT; (c) ratio between true outer fibre tensile stress σ and nominal bending stress versus nominal bending stress σ_{nom}, (d) comparison of nominal bending strength and true outer fibre tensile stress.

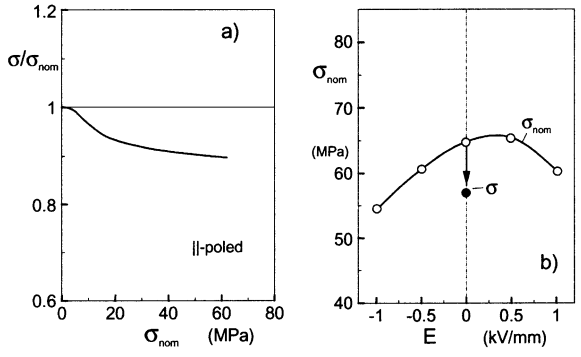

Fig. 7. (a) Ratio between true outer fibre tensile stress σ and nominal bending stress versus nominal bending stress σ_{nom}, (b) comparison of nominal bending strength arid true outer fibre tensile stress for $E=0$.

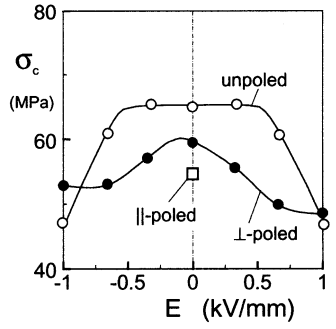

Fig. 8. Comparison of true bending strengths for the differently poled materials.

Table 1
Weibull parameters σ_0 for the conventionally computed bending strength and the true outer fibre tensile stress σ_0 at $E=0$ [results for short bars recalculated by Eq. (3)]

Material	$\sigma_{nom,0}$ (MPa)	σ_0 (MPa)
Unpoled [1,7]	82	64
⊥-Poled [1,7]	74	59
‖-Poled	60	54

unit cell in the domains with an orientation parallel or perpendicular to the stress axis.

4.2.1. Unpoled material

In the unpoled material, we will find one third of all domains orientated in the *x*-direction, one third in *y*-direction, and one third in *z*-direction (Fig. 9a). If a mechanical load is applied normal to the crack plane (strongly magnified near the crack tip), most of the domains will switch to the stress direction (Fig. 9b) with an anti-parallel orientation. The increase in domains in *y*-direction causes a residual stress field which reduces the influence of the externally applied stress. This is interpreted as an increase in the resistance against crack propagation (for references dealing with macroscopic cracks[12–14]).

4.2.2. Poling in the x*-direction*

In the case of the PZT being poled perpendicular to the stress direction, nearly all domains may be orientated in *x*-direction (Fig. 9c). Under tensile stresses, an orientation of the domains in the *y*-direction can also be observed, similar to the orientation of domains in the unpoled material (Fig. 9d).

While two thirds of all domains in unpoled material can switch to the *y*-direction, all domains are able to switch in the case of ⊥-poled PZT. Consequently, increased domain switching and increased strength must be expected. Domain switching from the poled state causes depolarisation, ΔP_x. This depolarisation is strongly concentrated in the vicinity of the crack tip. The highly stressed and depoled zone is in series with the nearly unstressed bulk material which remains in the poled state. Therefore, the short-circuited electrodes—far away from the depoled zone—are without any effect and the electric boundary conditions are given by a constant dielectric displacement, $D=$constant. An electric field, ΔE_x, is generated due to depoling

$$D_x = \varepsilon E_x + P_x = \text{constant} \Rightarrow \Delta E_x = -\Delta P_x/\varepsilon \qquad (6)$$

($\varepsilon=$dielectric permittivity), which inhibits depoling by domain switching (Fig. 9d), i.e. switching in the poled state needs a higher stress to reach the same degree of domains orientated in the *y*-direction. From the lower true strength σ_0 of the ⊥-poled material as compared to the unpoled PZT, we can conclude that the restricted ability of domain switching exceeds the effect of a larger reservoir of switchable domains.

4.2.3. Poling in the y*-direction*

In the ‖-poled case (Fig. 9e), the number of domains in *x*- and *z*-directions able to switch into the *y*-direction is very small. Therefore, we do not expect any effect of reorientation (Fig. 9f). Hence, the lower strengths of ‖-poled PZT can be understood.

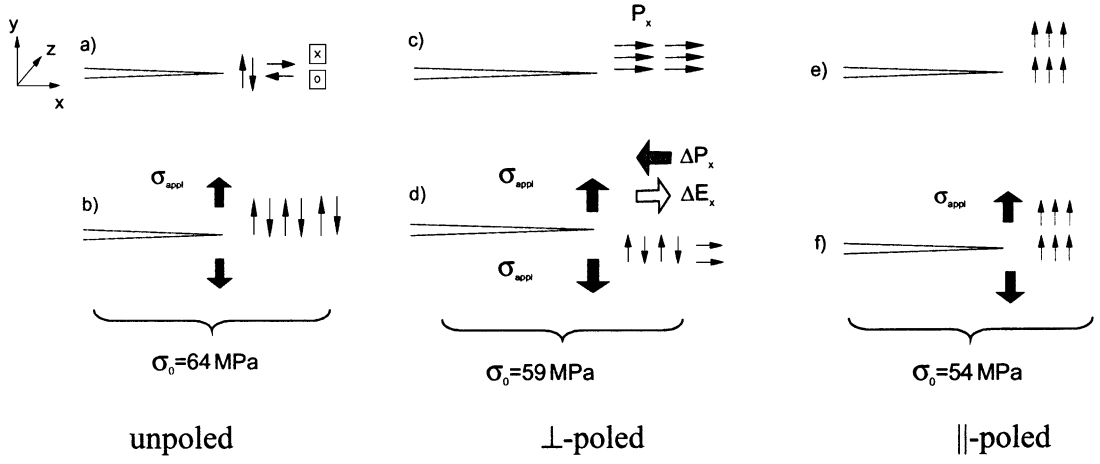

Fig. 9. Orientation of domains in front of a crack in an unpoled (a, b) a ⊥-poled (c, d), and a ‖ poled PZT caused by a mechanical load.

4.3. Influence of the electric field on strength

For all poling states, it becomes clear from Figs. 4 and 8 that strength decreases at high positive arid negative electric fields. A possible explanation may be given here.

4.3.1. Unpoled specimens

In Fig. 10a, we apply an electric field, E, in the direction of the crack plane (x-direction) for an unpoled PZT. In a high electric field (e.g. 1 kV/mm), most of the domains will switch into x-direction (with the same orientation sense). If the electric field and the applied stress are simultaneously present (Fig. 10b), free switching to y-direction is restrained. Therefore, the degree of reorientation is lower than in the case of $E=0$, although the number of domains oriented in the x-direction (able to switch) is larger. The number of domains is expected to be between the two limiting cases shown in Figs. 9b and 10b. In this case, we must expect a reduced strength.

As a consequence of an increasing electric field with its increasing support of the polarisation generated, a decrease in toughness and strength must be expected. This prediction is in agreement with the measurements shown in Fig. 10c.

4.3.2. ⊥-Poled specimens

The behaviour of the ⊥-poled material under an electric field parallel to polarisation (Fig. 11a) can be explained in the same way as of the poled material in the absence of an external field. The internal electric field, ΔE_x, caused by depolarisation of the zone near the tip is effectively increased by the applied field and acts in the same direction. Consequently, domain switching is inhibited (Fig. 11b), and the strength is lower than in the case of $E=0$ (Fig. 11c).

Application of a moderate antiparallel electric field enhances depolarisation under transverse tensile stresses, as can be seen from Fig. 12b. The resulting strength

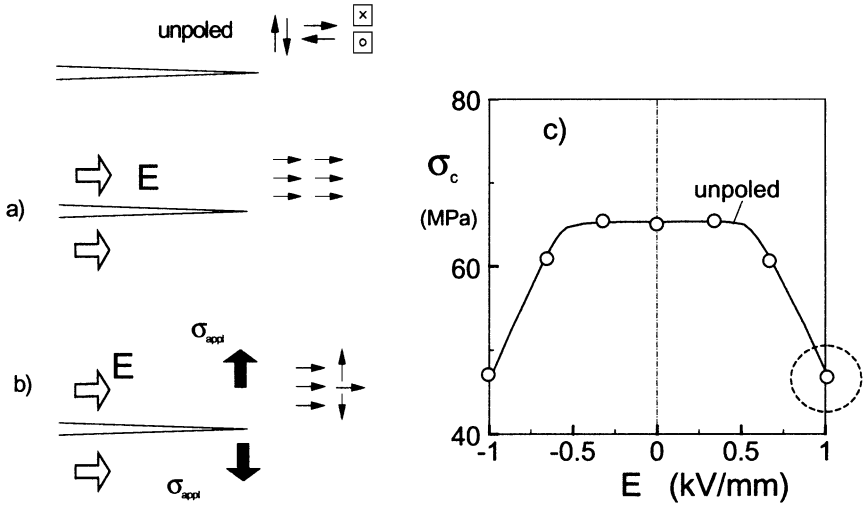

Fig. 10. Influence of combined mechanical stress σ_{appl} and electric field E on the domains in front of a crack for unpoled PZT.

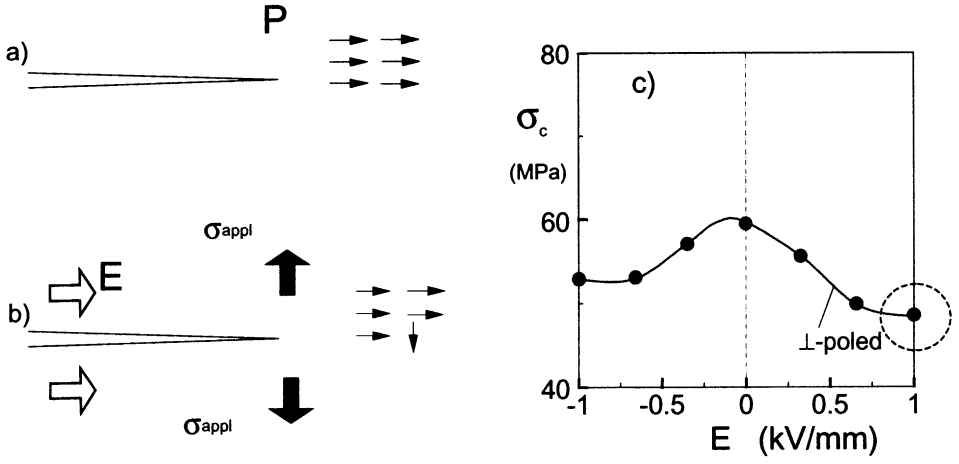

Fig. 11. Influence of mechanical stress and a positive electric field, E, on the domains for ⊥-poled PZT.

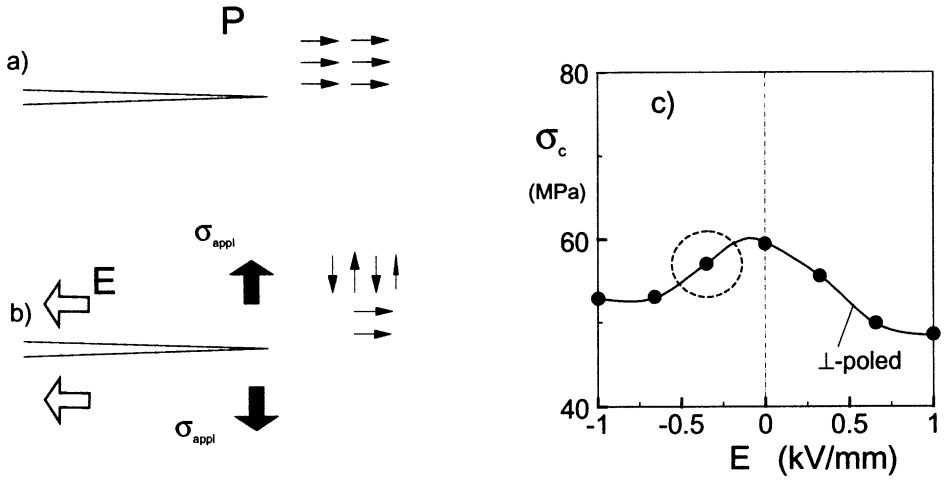

Fig. 12. Influence of a moderate negative electric field, E, on the domains for ⊥-poled PZT.

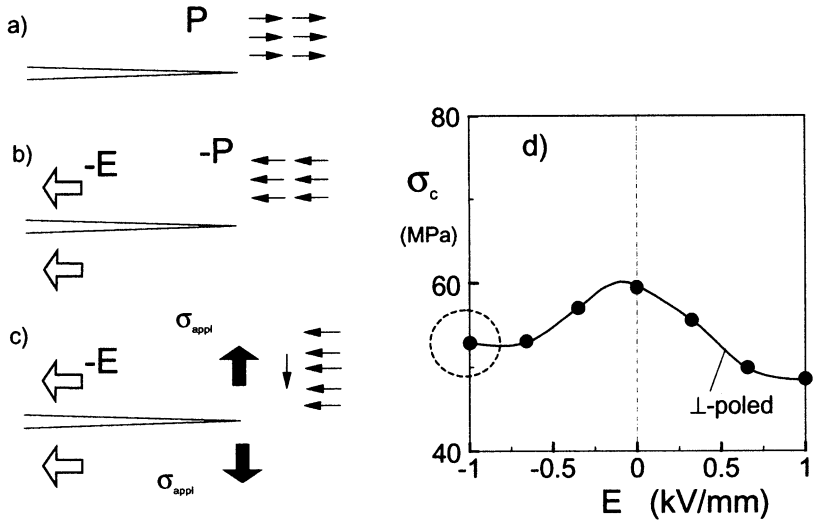

Fig. 13. Influence of a strong negative electric field.

(Fig. 12c) is higher than that obtained in the case of a positive electric field (Fig. 11c).

Fig. 13a again shows the poled material state. Under strong negative fields, the material will be repoled completely in the negative direction (Fig. 13b). The amount of domain switching (Fig. 13c) and the related strength values then must be comparable to the strengths under strong positive fields. This decrease of strength is in agreement with the experimental results shown in Fig. 13d.

5. Summary

Bending strength measurements were performed on a soft PZT in different poling states in the presence of electric fields. The nominal bending strength data (defined by the ratio of bending moment and moment of inertia) were transformed into true outer fibre bending strengths by use of the Nadai procedure. The main results were:

- In the absence of an electric field, we found the ranking of

$$\sigma_{c,\parallel} < \sigma_{c,\perp} < \sigma_{c,\text{unpoled}}$$

- At strong electric fields ($E = \pm 1$ kV/mm), the strengths (nominal and true bending strength) are significantly smaller than in the absence of an electric field.
- Only a slight non-symmetry of strength data is found with respect to the field direction.

The influences of the poling state and of the external electric field are discussed in terms of the orientation of domains in front of natural cracks.

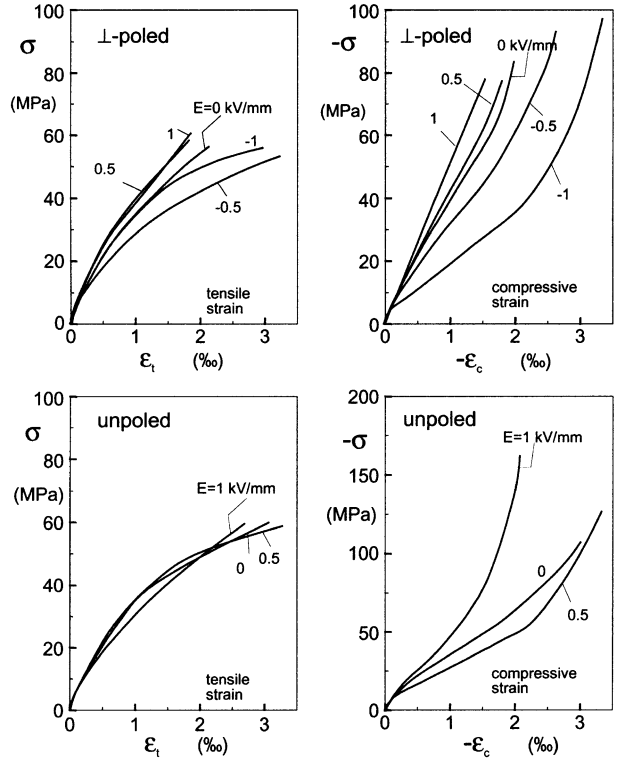

Fig. 14. Stress-strain curves obtained from bonding tests by application of the Nadai procedure [10,11].

Appendix

Stress–strain curves obtained from bending tests by application of the Nadai procedure[10,11] are plotted below.

References

1. Fett, T., Munz, D. and Thun, G., Strength of a soft PZT ceramic under a transversal electric field. *J. Mater. Sci. Letters*, 2000, **19**, 1921–1924.
2. Zhang, T. Y. and Zhao, M., Fracture of piezoelectric materials. International Conference on Fracture, ICF 10, Honolulu, December 2001, Contribution No 0404.
3. Fu, R. and Zhang, T. Y., Influences of temperature and electric field on the bending strength of lead zirconate titanate ceramics. *Acta Mater.*, 2000, **48**, 1729–1740.
4. Makino, H. and Kamiya, N., Effect of dc electric field on mechanical properties of piezoelectric ceramics. *Jpn. J. Appl. Phys.*, 1994, **33**, 5323–5327.
5. Zhang, T. Y., Zhao, M. H. and Tong, P., Fracture of piezoelectric ceramics. *Advances in Applied Mechanics*, 2001, **38**, 147–289.
6. Fett, T., Munz, D. and Thun, G., Differences in bending and tensile strength for soft PZT. *Proceedings 9th Cimtec*, 1998, **(Part E)**, 299–306.
7. Fett, T. and Munz, D., Measurement of Young's moduli for lead zirconate titanate (PZT) ceramics. *J. Testing and Evaluation*, 2000, **28**, 27–35.
8. Thoman, D. R., Bain, L. J. and Antle, C. E., Inferences on the parameters of the Weibull distribution. *Technometrics*, 1969, **11**, 445.
9. Munz, D. and Fett, T., *Ceramics*. Springer Verlag, Heidelberg, Germany, 1999.
10. Nadai, A., *Theory of Flow and Fracture of Solids* (chapter 22), Vol. 1. McGraw-Hill, New York, 1950.
11. Fett, T., Munz, D. and Thun, G., Nonsymmetric deformation behaviour of PZT determined in bending tests. *J. Am. Ceram. Soc.*, 1998, **81**, 269–272.
12. Schneider, G. A. and Heyer, V., Influence of the electric field on Vickers indentation crack growth in $BaTiO_3$. *J. Eur. Ceram. Soc.*, 1999, **19**, 1299–1306.
13. Chen, W. and Lynch, C. S., A micro-electro-mechanical model for polarization switching of ferroelectric materials. *Acta Mater.*, 1998, **46**, 5303–5312.
14. Fett, T., Kamlah, M., Munz, D. and Thun, G., Strength of a PZT ceramic under different test conditions. *SPIE's 7th Int. Symp. on Smart Structures and Materials*, Newport Beach, USA, 2000.